



Article

Obtaining of Mg-Zn Co-Doped GaN Powders via Nitridation of the Ga-Mg-Zn Metallic Solution and Their Structural and Optical Properties

Erick Gastellóu ^{1,2,*} , Rafael García ², Ana M. Herrera ², Antonio Ramos ², Godofredo García ³, Gustavo A. Hirata ⁴, José A. Luna ³ , Roberto C. Carrillo ⁵ , Jorge A. Rodríguez ¹ , Mario Robles ¹, Yani D. Ramírez ⁶ and Guillermo Martínez ⁷ 

- ¹ División de Sistemas Automotrices, Universidad Tecnológica de Puebla (UTP), Antiguo Camino a la Resurrección 1002–A, Zona Industrial, Puebla 72300, Puebla, Mexico
 - ² Departamento de Investigación en Física, Universidad de Sonora (UNISON), Rosales y Colosio, C. De la Sabiduría, Centro, Hermosillo 83000, Sonora, Mexico
 - ³ Centro de Investigación en Dispositivos Semiconductores, Benemérita Universidad Autónoma de Puebla (BUAP), 14 Sur y Av. San Claudio, Puebla 72570, Puebla, Mexico
 - ⁴ Centro de Nanociencias y Nanotecnología, Universidad Nacional Autónoma de México (UNAM), Carr. Tijuana-Ensenada km107, C.I.C.E.S.E., Ensenada 22860, Baja California, Mexico
 - ⁵ Departamento de Física, Universidad de Sonora (UNISON), Rosales y Colosio, C. De la Sabiduría, Centro, Hermosillo 83000, Sonora, Mexico
 - ⁶ Departamento de Investigación y Desarrollo, Universidad Tecnológica de Puebla (UTP), Antiguo Camino a La Resurrección 1002–A, Zona Industrial, Puebla 72300, Puebla, Mexico
 - ⁷ Departamento de Ingeniería Química, Universidad de Guanajuato (UGTO), Noria Alta S/N, Guanajuato 36050, Guanajuato, Mexico
- * Correspondence: erick_gastellou@utpuebla.edu.mx; Tel.: +52-2224699594



Citation: Gastellóu, E.; García, R.; Herrera, A.M.; Ramos, A.; García, G.; Hirata, G.A.; Luna, J.A.; Carrillo, R.C.; Rodríguez, J.A.; Robles, M.; et al. Obtaining of Mg-Zn Co-Doped GaN Powders via Nitridation of the Ga-Mg-Zn Metallic Solution and Their Structural and Optical Properties. *Materials* **2023**, *16*, 3272. <https://doi.org/10.3390/ma16083272>

Academic Editor: Rene A. Castro Arata

Received: 2 March 2023

Revised: 29 March 2023

Accepted: 7 April 2023

Published: 21 April 2023



Copyright: © 2023 by the authors. Licensee MDPI, Basel, Switzerland. This article is an open access article distributed under the terms and conditions of the Creative Commons Attribution (CC BY) license (<https://creativecommons.org/licenses/by/4.0/>).

Abstract: Mg-Zn co-doped GaN powders via the nitridation of a Ga-Mg-Zn metallic solution at 1000 °C for 2 h in ammonia flow were obtained. XRD patterns for the Mg-Zn co-doped GaN powders showed a crystal size average of 46.88 nm. Scanning electron microscopy micrographs had an irregular shape, with a ribbon-like structure and a length of 8.63 μm. Energy-dispersive spectroscopy showed the incorporation of Zn (L α 1.012 eV) and Mg (K α 1.253 eV), while XPS measurements showed the elemental contributions of magnesium and zinc as co-dopant elements quantified in 49.31 eV and 1019.49 eV, respectively. The photoluminescence spectrum showed a fundamental emission located at 3.40 eV (364.70 nm), which was related to band-to-band transition, besides a second emission found in a range from 2.80 eV to 2.90 eV (442.85–427.58 nm), which was related to a characteristic of Mg-doped GaN and Zn-doped GaN powders. Furthermore, Raman scattering demonstrated a shoulder at 648.05 cm⁻¹, which could indicate the incorporation of the Mg and Zn co-dopants atoms into the GaN structure. It is expected that one of the main applications of Mg-Zn co-doped GaN powders is in obtaining thin films for SARS-CoV-2 biosensors.

Keywords: co-doped; GaN; nitridation; liquid metallic solution; semiconductors

1. Introduction

The semiconductor supply chain (SSC) is very important nowadays and is vital in the industry's demand, such as computers, communication, consumer, automotive, and government. The SARS-CoV-2 pandemic had devastating effects on SSC, generating a shortage in the semiconductor industry, besides increased prices in electronic devices [1]. Currently, the semiconductor industry is beginning to activate, where some of the materials more affected have been the III-nitride compounds. Gallium nitride (GaN) is one of the more important binary III-nitride compounds, with structural and optical properties, whose characteristics are continuing to improve through research. The doping of the GaN is attractive owing to changes in the mobility of charge carriers. GaN has applications in full-color

displays, GaN-based power devices, Schottky barrier diodes, light-emitting diodes, high-electron-mobility transistors, piezoelectric MEMs, and solar cells [2–4]. Other applications could be in laser devices for optical communications; medicine; and industry [5–9].

In recent years, the strategies of doping and of defect control have regained their importance in semiconductor physics for researchers. Co-doping is an important strategy used for tuning the dopant in electronic and magnetic properties, besides enhancing dopant solubility, and increasing activation by lowering the ionization energy of acceptors and donor, thus increasing the carrier's mobility [10,11]. In P-type GaN, the Mg-H co-doped is one of the best examples of fully compensated co-doping [11]. K.H. Ploog investigated the Be-O co-doped GaN with a strongly improved P-type conductivity at room temperature due to the substantial enhancement of the hole-mobility [12]. On the other hand, R.Y. Korotkov et al. investigated Mg-O co-doped GaN, obtaining hole concentrations of $2 \times 10^{18} \text{ cm}^{-3}$ at 295 K, with resistivity from 8 to $0.2 \text{ } \Omega\text{cm}$ [13]. In another work, H. Pan et al. showed a novel application of photocatalytic activity in the visible light region realized with Cr-O co-doped GaN [14]. P-type GaN can be obtained by incorporating divalent elements such as Zn, Be, and Mg, where the co-doping of two different dopants could produce a low resistivity P-type GaN. K.S. Kim et al. showed the obtaining of Mg-Zn co-doped GaN grown by MOCVD, showing a P-type GaN with low electrical resistivity of $0.72 \text{ } \Omega\text{cm}$ and a high hole concentration of $8.5 \times 10^{17} \text{ cm}^{-3}$ [15,16]. In general, there is poor research in the literature regarding the Mg-Zn co-doped GaN material.

This investigation shows the synthesis of Mg-Zn co-doped GaN powders via the nitridation of the Ga-Mg-Zn metallic solution in ammonia flow at $1000 \text{ } ^\circ\text{C}$ for 2 h, which could have application in the deposit of thin films by RF magnetron sputtering using laboratory-prepared targets. This is a way of contributing to research on the co-doping of GaN with Mg-Zn. To compare the results obtained of Mg-Zn co-doped GaN powders, undoped GaN powders were obtained by the nitridation of metallic gallium, as was reported in our before studies [17]. On the other hand, the characterizations X-ray diffraction patterns (XRD), scanning electron microscopy (SEM), energy-dispersive spectroscopy (EDS), X-ray photoelectron spectroscopy (XPS), transmission electron microscopy (TEM), photoluminescence (PL), and Raman scattering were carried out to know the structural and optical properties of the Mg-Zn co-doped GaN powders.

2. Materials and Methods

Mg-Zn co-doped GaN powders were synthesized using metallic gallium (99.999%), metallic magnesium, and metallic Zn as reagents. Moreover, as the source of nitrogen atoms, ammonia (NH_3) was used. To obtain the Mg-Zn co-doped GaN, the powders were used 1.32 g of metallic gallium (19.02 mmol), 5.20 mg of metallic magnesium ($0.21 \text{ mmol} \cong 0.4\%$), and 7.80 mg of metallic zinc ($0.12 \text{ mmol} \cong 0.6\%$). To obtain the undoped GaN powders, 3.37 g (48.41 mmol) of metallic gallium was used, following the process realized in our before work [18]. The reaction formulated to obtain the Mg-Zn co-doped GaN material is the following [17]:



2.1. Mg-Zn Co-Doped GaN Powders

To begin the process of synthesis of Mg-Zn co-doped GaN powders, the general preparation of the metallic solution was carried out according to the work of Gastellou et al. [18]. Once obtained, the metallic solution was introduced inside a chemical vapor deposition furnace (CVD), whereupon the CVD system was purged, and later an N_2 flow at 50 sccm was opened and was allowed to flow into the atmosphere. After, to ensure the diffusion of Zn atoms into the gallium of the Ga-Zn liquid solution, the temperature was increased to $440 \text{ } ^\circ\text{C}$ for 40 min [18,19]. On the other hand, to ensure the diffusion of Mg atoms into the metallic gallium of the Ga-Mg-Zn metallic solution, the temperature was increased to $670 \text{ } ^\circ\text{C}$ for 40 min ($20 \text{ } ^\circ\text{C}$ above the Mg melting point) [20,21]. Later, once the temperature

had been stabilized at 670 °C and 40 min has passed, the N₂ flow was closed, and an NH₃ flow at 150 sccm was introduced inside the furnace. At this moment, the temperature of the Ga-Mg-Zn metallic solution was increased to 900 °C for 40 min for its homogenization process (first stage), and finally the Ga-Mg-Zn metallic solution was increased to 1000 °C for 2 h for its nitridation process (second stage). After the nitridation process was finished, the ammonia flow was closed; then, the temperature was decreased to room temperature using an N₂ flow at 150 sccm to cool the system. The synthesized material was taken out of the furnace and ground to obtain Mg-Zn co-doped GaN powders.

The synthesis does not require a cleaning process due to the fact the Mg atoms and Zn atoms were defunded in the Ga metallic and transformed into the final material. The total weight synthesized of Mg-Zn co-doped GaN powders was 1.5661 g (9.02 mmol), which indicates that there was a nitrogen incorporation of 233.10 mg (16.65 mmol). A diagram of the synthesis process is shown in Figure 1, while Table 1 shows the parameters considered in the synthesis of Mg-Zn co-doped GaN powders.

Table 1. Parameters considered in the synthesis of Mg-Zn co-doped GaN powders.

Ga Weight (g)	Mg Weight (mg)	Zn Weight (mg)	Zn Homogenization Temperature (°C)	Mg Homogenization Temperature (°C)	Nitridation Temperature (°C)	Nitridation Time (h)
1.32	5.20	7.80	440	670	1000	2

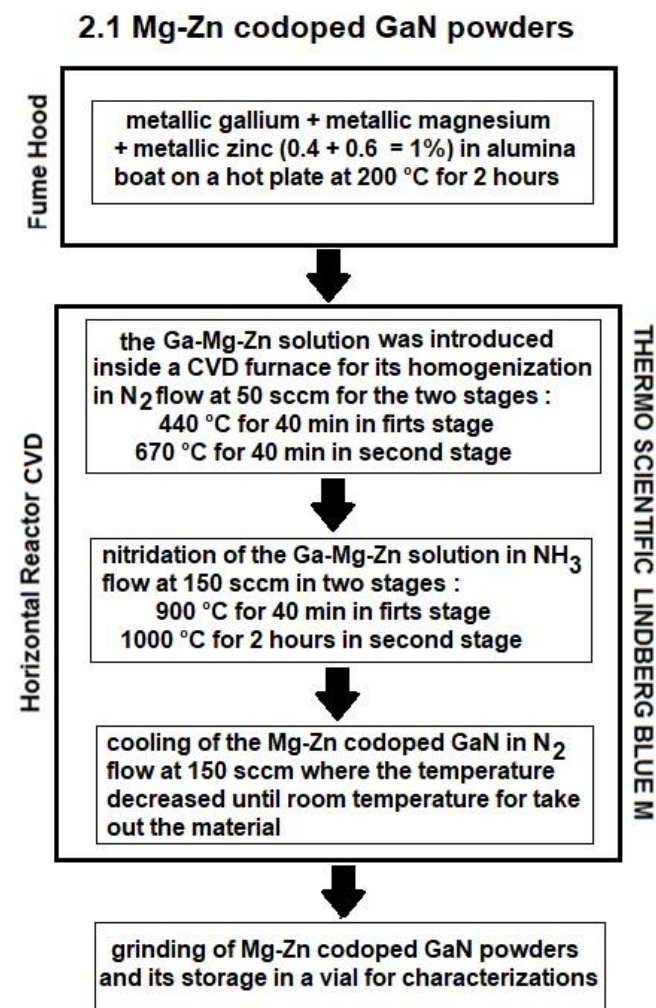


Figure 1. Diagram to obtain the Mg-Zn co-doped GaN powders.

2.2. Characterizations

The Mg-Zn co-doped GaN and undoped GaN powders were characterized by X-ray diffraction (XRD) using a Philips X'PERT MPD equipment with a wavelength (Cu K α) of 1.5406 Å. The measurements of XRD patterns were realized with a range from 30° to 60°. The surface morphology and the elemental analysis (SEM/EDS) of the Mg-Zn co-doped GaN, and of the undoped GaN powders, were obtained using JEOL JSM-7800F Schottky Field Emission equipment. X-ray photo-electron spectroscopy (XPS) characterizations were carried out using an Escalab 250Xi Brochure equipment with an energy range from 0 to 1400 eV for the Mg-Zn co-doped GaN powders. Transmission electron microscopy (TEM) was obtained using JEOL JEM-2010 equipment for the Mg-Zn co-doped GaN and the undoped GaN powders. Photoluminescence spectra (PL) were measured at room temperature with an excitation wavelength of 325 nm (UV) and a power of 55 mW, using an IK series He–Cd LASER for the Mg-Zn co-doped GaN, and undoped GaN powders. Finally, the Raman scattering characterizations for the Mg-Zn co-doped GaN and the undoped GaN powders were obtained using a Horiba Jobin Yvon HR-800 Micro Raman spectrophotometer.

3. Results and Discussion

3.1. Structure

Figure 2 shows a comparison between the XRD patterns of the undoped GaN powders (Figure 2a), and the Mg-Zn co-doped GaN powders (Figure 2b). In Figure 2, all of the peaks of both X-ray diffraction patterns were indexed in the ICDD pdf card: 00-050-0792. The **a** peak was found at plane orientation (100), **b** at (002), **c** at (101), **d** at (102), and **e** at (110). The lattice constants $a = 3.1890$ Å and $c = 5.1855$ Å were calculated for the hexagonal structure, with a ratio c/a of 1.626 belonging to space group $P6_3mc(186)$. Nitrides oxide or pure metals were not detected, indicating the adequate diffusion of the co-dopants of Mg-Zn into GaN powders. Moreover, Figure 2 shows that there is no a significant difference between the diffraction patterns Figure 2a,b. Both diffraction patterns showed narrowed peaks, which could indicate the presence of large crystals in both samples. FWHM measurements were carried out for the X-ray diffraction pattern of Figure 2b; the (100) plane orientation had 0.1634°, 0.1708° for (002), 0.1786° for (101), 0.2130° for (102), and 0.2424° for (110). Table 2 shows the measurements for peak position, FWHM, crystal size, and interplanar spacing for Figure 2a,b. Calculations of the displacement of the Figure 2b in relation to Figure 2a based on Table 2 were carried out, finding a displacement to the right. The **a** peak had a displacement of 0.0493°, the **b** peak of 0.0527°, the **c** peak of 0.0513°, the **d** peak of 0.0527°, and the **e** peak of 0.0486°. Using the ICCD PDF-4+ 2022 software and the Debye-Scherrer [22], the crystal size had a value of 48.61 nm for the undoped GaN powders and 46.88 nm for the Mg-Zn co-doped GaN powders.

Table 2. Values calculated for peak position, FWHM, crystal size, and interplanar spacing for undoped GaN and Mg-Zn co-doped GaN powders.

Peak	Undoped GaN Powders				Mg-Zn Co-Doped GaN Powders			
	Peak Position (Degree)	FWHM (Degree)	Crystal Size (nm)	Interplanar Spacing (Å)	Peak Position (Degree)	FWHM (Degree)	Crystal Size (nm)	Interplanar Spacing (Å)
a	32.3247	0.1697	50.8913	2.7672	32.3740	0.1634	52.8691	2.7631
b	34.4971	0.1615	53.7662	2.5978	34.5498	0.1708	50.8475	2.5939
c	36.7747	0.1742	50.1737	2.4419	36.8260	0.1786	48.9618	2.4386
d	48.0318	0.1956	46.4284	1.8926	48.0845	0.2130	42.6433	1.8907
e	57.7078	0.2266	41.7941	1.5962	57.7565	0.2424	39.0862	1.5949

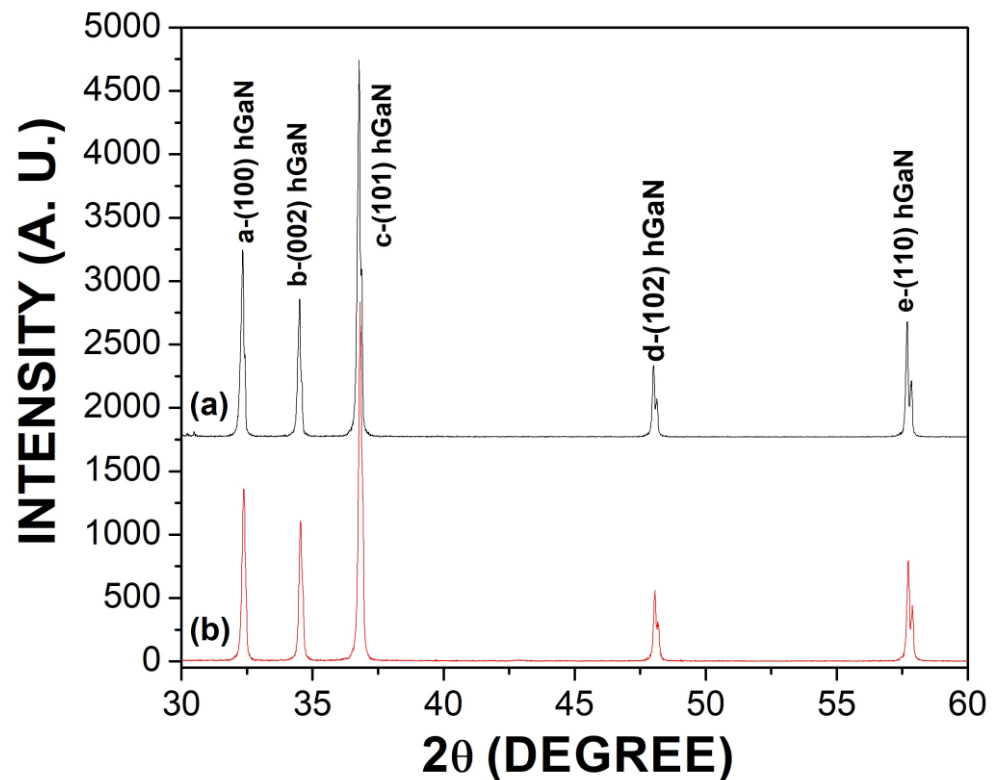


Figure 2. (a) XRD pattern of the undoped GaN powders; (b) XRD pattern of the Mg-Zn co-doped GaN powders.

3.2. Electron Microscopy

Figure 3a shows the surface morphology of the undoped GaN, which demonstrated hexagonal crystals for the micrograph at $2500\times$, whose values were $20.76\ \mu\text{m}$ in width and $23.16\ \mu\text{m}$ in length. Moreover, the micrograph at $5000\times$ also showed hexagonal crystals of different sizes with values of $6.28\ \mu\text{m}$ in width and 7.80 in length. On the other hand, Figure 3b showed the surface morphology of the Mg-Zn co-doped GaN powders, which had an irregular shape with a ribbon-like structure with an average length of $8.63\ \mu\text{m}$. The surface morphology of the ribbon-like structure of the Figure 3b could be related to the Mg and Zn incorporation via diffusion into the GaN. It is possible that during the formation of the ribbon-like structure, oxygen or carbon interstitial atoms are desorbed of the GaN structure, whereupon magnesium or zinc replace the vacancies; this way, the co-doping with Mg and Zn into the GaN structure is carried out.

Figure 4a presents the energy dispersive spectroscopy (EDS) spectrum corresponding to Figure 3a, which demonstrated the elemental contributions of gallium and nitrogen; besides copper belonging to the sample holder, there are few traces of non-intentional impurities of oxygen and carbon. Figure 4b shows the EDS spectrum corresponding to Figure 3b, which showed the elemental contributions of gallium ($K\alpha$ 9.241 eV and $L\alpha$ 1.098 eV), and nitrogen ($K\alpha$ 0.392 eV). Figure 3b also showed few traces of oxygen and carbon. It is important to mention that Figure 3b demonstrated the presence of zinc ($L\alpha$ 1.012 eV) and magnesium ($K\alpha$ 1.253 eV), with atomic percentages of 0.60% and 0.32%, respectively. Furthermore, the atomic percentages for gallium and nitrogen of Figure 3b were 49.66% and 31.81%, respectively.

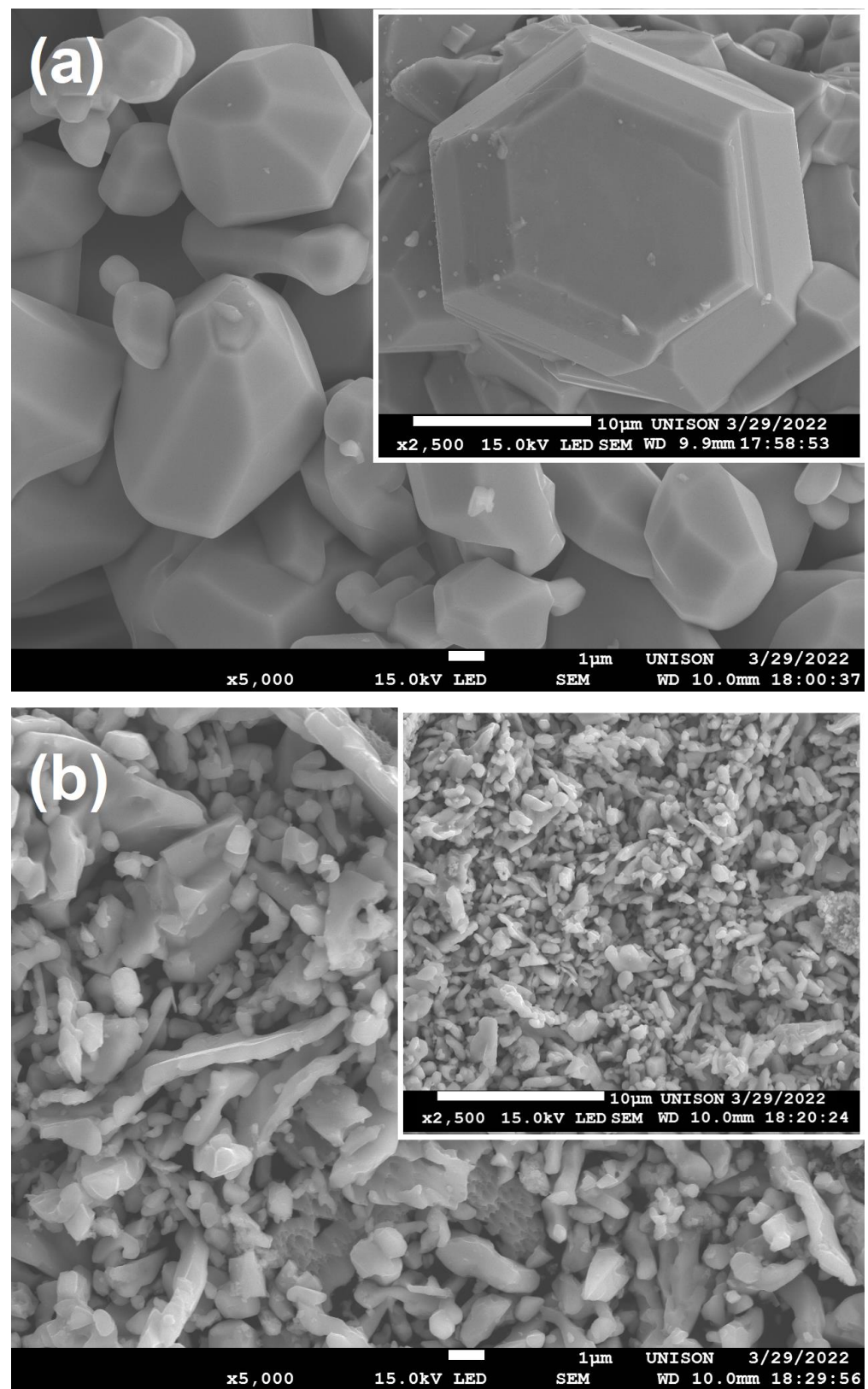


Figure 3. (a) SEM micrographs of the undoped GaN powders; (b) SEM micrographs of the Mg-Zn co-doped GaN powders.

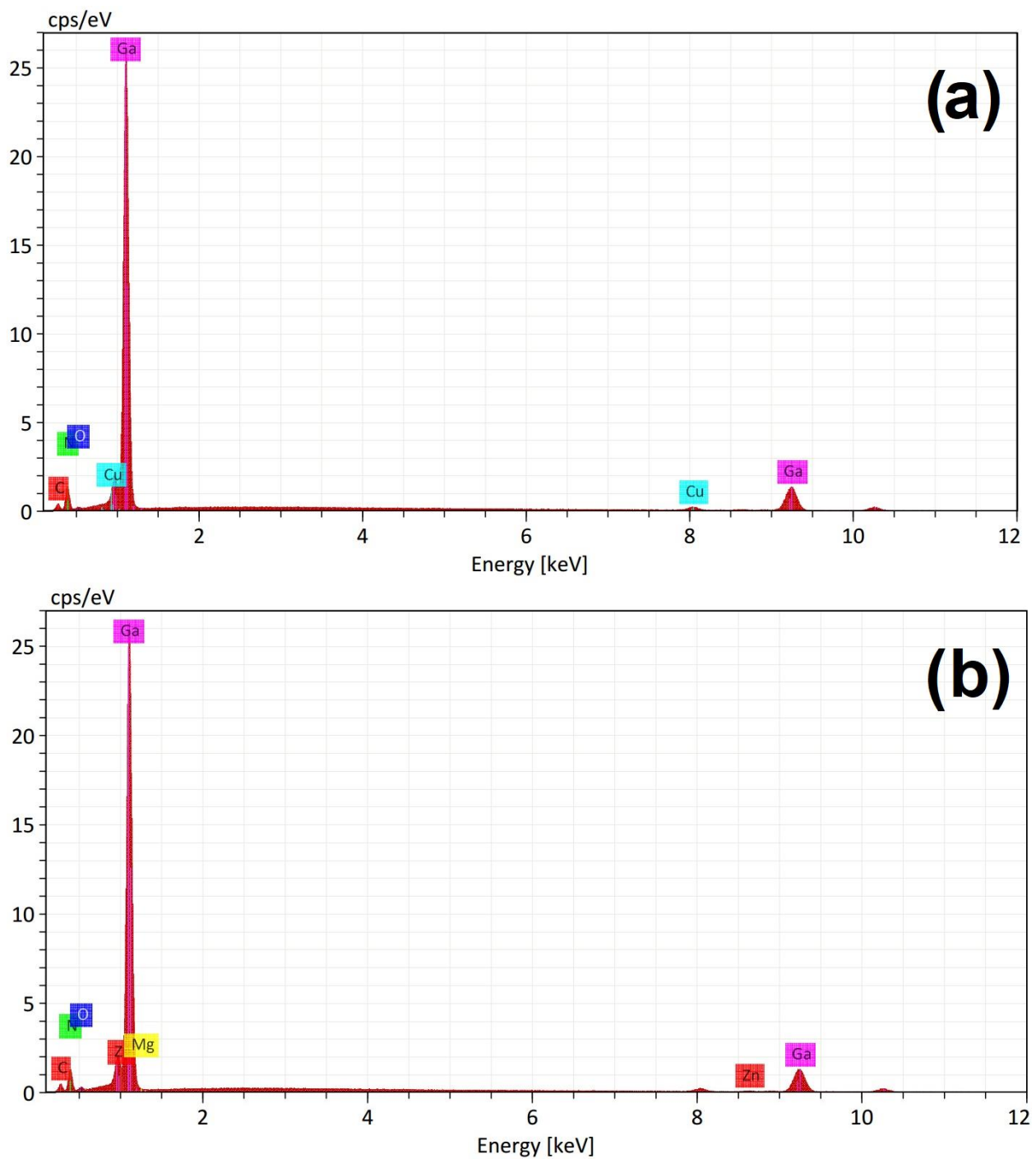


Figure 4. (a) EDS spectrum of SEM image of Figure 3a for the undoped GaN powders, (b) EDS spectrum of SEM image of Figure 3b for the Mg-Zn co-doped GaN powders.

Figure 5a shows the TEM micrograph of the sample of Mg-Zn co-doped GaN powders, which had values of 496.5 nm in width and 606.8 nm in length, for a magnification at 200 nm. Figure 5b shows the electron diffraction pattern for the undoped GaN powders, which can be observed as a distribution uniform of GaN atoms. However, Figure 5c showed the electron diffraction pattern for the Mg-Zn co-doped GaN powders, where a greater scattering of impurities or co-dopant atoms in the GaN sample was observed. This scattering of impurities might indicate the incorporation of the diffusion of Mg and Zn atoms into GaN, which agrees with the ribbon-like structure in Figure 3b and the EDS spectrum in Figure 4b.

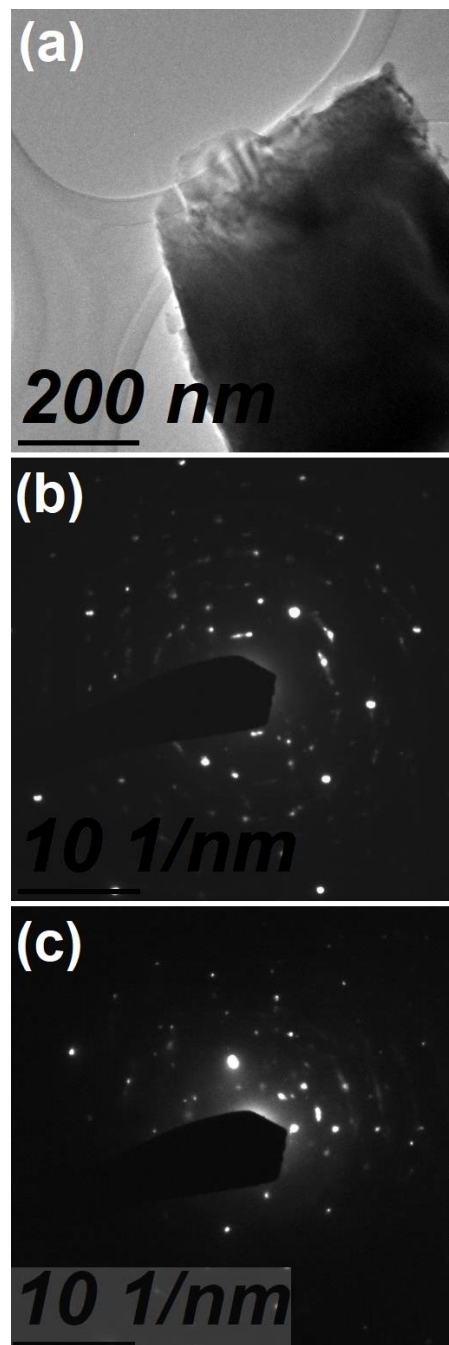


Figure 5. (a) TEM micrograph of the sample of Mg-Zn co-doped GaN powders, (b) electron diffraction pattern of the undoped GaN powders, and (c) electron diffraction pattern of the Mg-Zn co-doped GaN powders.

3.3. X-ray Photo-Electron Spectroscopy

Figure 6 presents the XPS spectra of the Mg-Zn co-doped GaN powders. Figure 6a presents the peaks for high energies of Ga $2P_{1/2}$ and Ga $2P_{3/2}$, with values of 1146.28 eV and 1119.76 eV, respectively. Figure 6b depicts the N 1s peak with an energy value of 399.29 eV. Figure 6c shows the Zn $2P_{3/2}$ peak with an energy value of 1019.49 eV, whose binding energy belongs to L_3 level. Figure 6d depicts the Mg $2P_{3/2}$ peak with a binding energy of 49.31 eV. It is important to mention that during the obtaining process of the Mg-Zn co-doped GaN powders, it was attempted to reduce the presence of oxygen and carbon, which can act as non-intentional impurities. However, Figure 6e shows the elemental contribution of the O 1s peak with a binding energy of 532.72 eV, and the Figure 6f shows

the presence of the elemental contribution of C 1s with a value of 285.68 eV, which could affect the optical properties of Mg-Zn co-doped GaN.

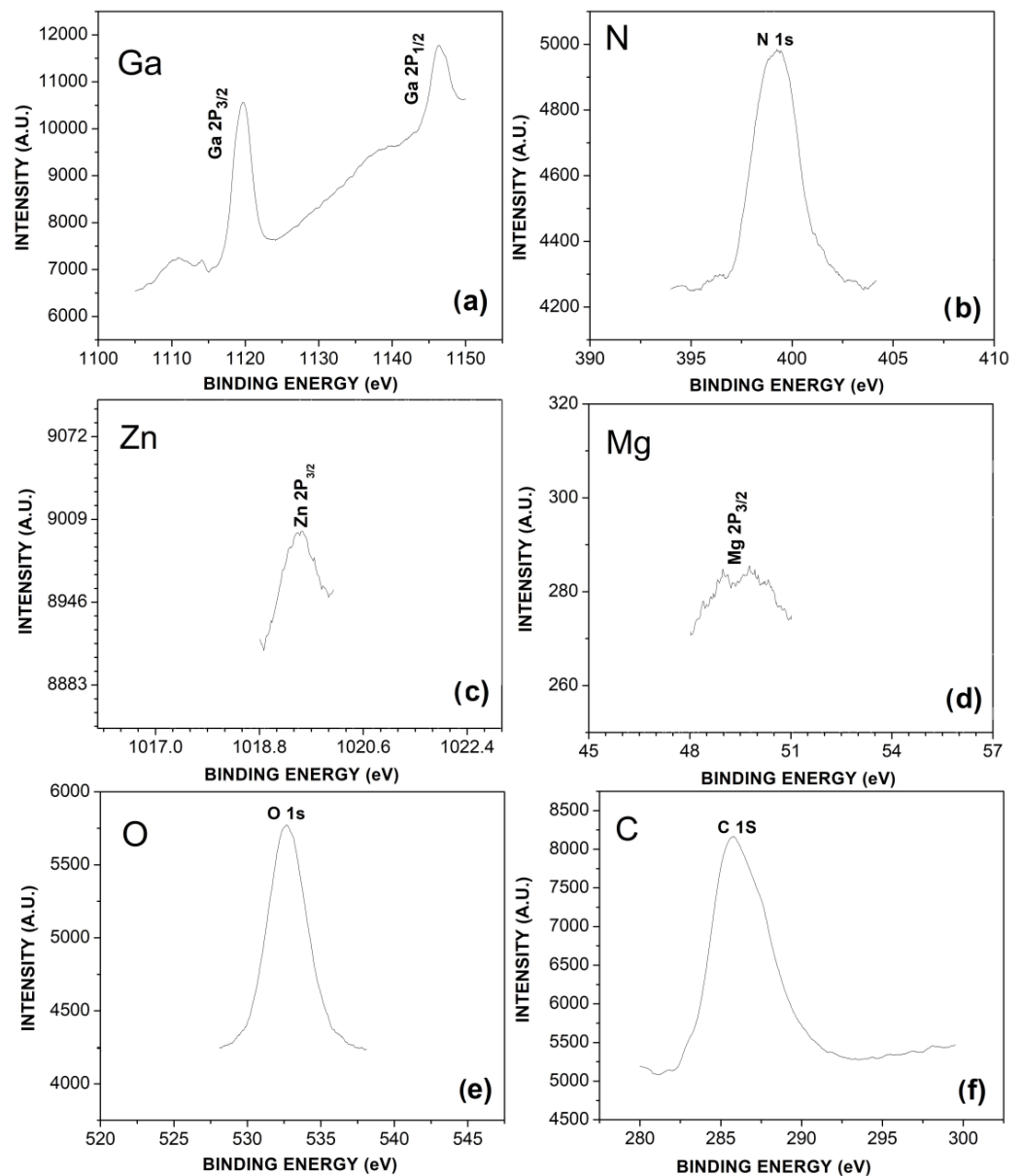


Figure 6. XPS spectra of the Mg-Zn co-doped GaN powders: (a) Ga 2P_{3/2} and Ga 2P_{1/2}, (b) N 1s, (c) Zn 2P_{3/2}, (d) Mg 2P_{3/2}, (e) O 1s, and (f) C 1s peaks.

3.4. Photoluminescence

Figure 7 shows the PL spectrum of the undoped GaN powders (black curve) and the PL spectrum of the Mg-Zn co-doped GaN powders (red curve). The **a** peak depicts high emission located at 3.40 eV (364.70 nm) due to the band-to-band transition, which corresponds to the ultraviolet emission for the hexagonal GaN. The **b** peak had an emission band located at 3.34 eV (371.25 nm) corresponding to the undoped GaN powders, which had been observed in samples with excitons bound to structural defects of GaN, perhaps related to the high concentration of stacking faults [23]. The **c** peak corresponds to the blue emission band located in a range from 2.80 eV to 2.90 eV (442.85–427.58 nm), which is characteristic of magnesium-doped GaN and zinc-doped GaN [24,25]. Figure 8 shows the decomposition of the **c** peak, where it is possible to observe the emission of 2.90 eV (**g** peak) related to magnesium-doped GaN. Furthermore, Figure 8 also shows the emission of 2.80 eV (**h** peak) related to zinc-doped GaN. The **d** peak was located in a yellow emission

band with an energy of 2.22 eV (558.14 nm) for the undoped GaN powders, which was related to Ga vacancies (V_{Ga}) and the substitutional atoms of carbon or oxygen (Figure 3a), indicating the obtaining of N-type GaN. On the other hand, the yellow emission band for the Mg-Zn co-doped GaN powders was null due to the P-type GaN samples [25]. The *e* peak had an emission with energy located at 1.70 eV (729.41 nm). This red emission band has been observed in heavily Mg-doped P-type GaN [23]. Finally, the *f* peak showed an emission in the red part of the spectrum at 1.67 (742.51 nm), which has been observed in Ga-lean samples. Figure 9a shows the yellow luminescence in undoped GaN powders, while Figure 9b shows the violet-blue luminescence of the Mg-Zn co-doped GaN powders, which were obtained with the excitation of a UV lamp “Blak-Ray UVL-56 (366 nm)”.

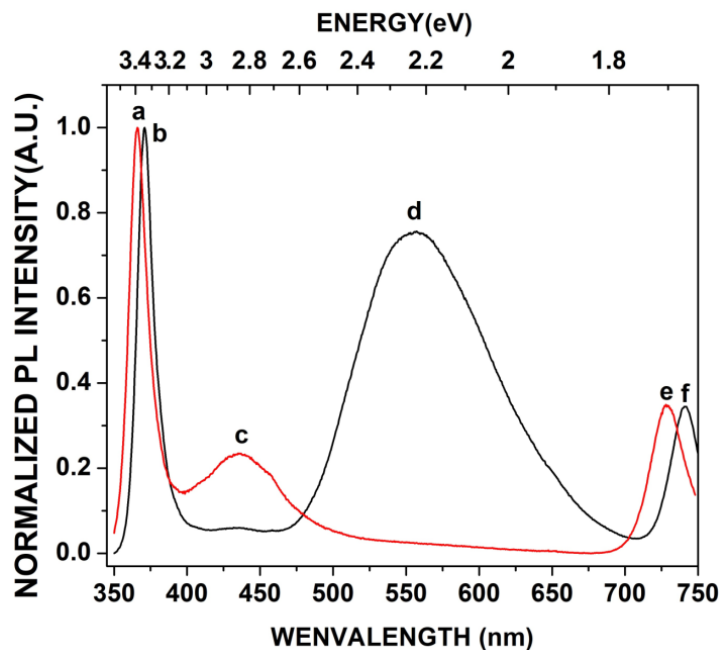


Figure 7. Photoluminescence spectra of the undoped GaN powders and the Mg-Zn co-doped GaN powders (a–f).

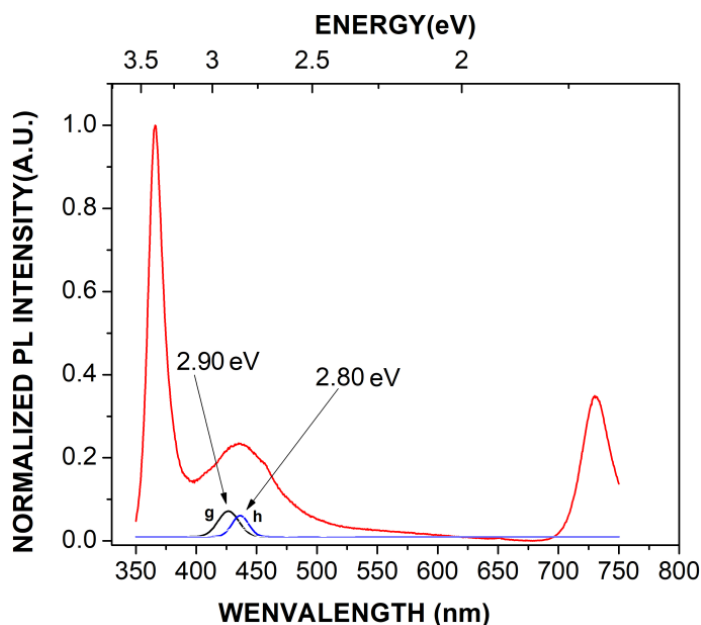


Figure 8. Decomposition of the *c* peak of the photoluminescence spectrum of the Mg-Zn co-doped GaN powders of Figure 7.

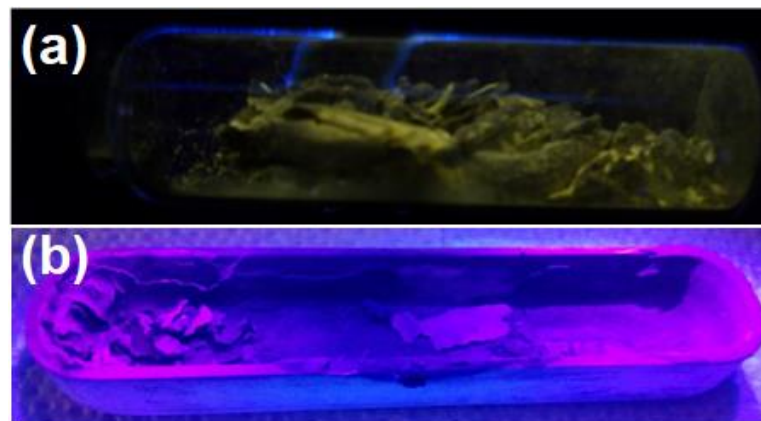


Figure 9. (a) Yellow luminescence of the undoped GaN powders; (b) violet-blue luminescence of the Mg-Zn co-doped GaN powders.

3.5. Raman Scattering

Figure 10a shows the Raman spectrum for the undoped GaN powders (red curve), and Figure 10b shows the Raman spectrum for the Mg-Zn co-doped GaN powders (black curve). Both Raman spectra show the classical vibration modes $A_1(\text{TO})$ and $E_2(\text{high})$ for the hexagonal GaN structure. However, the Raman spectrum for the Mg-Zn co-doped GaN powders also showed the vibration mode $E_2(\text{low})$. The $E_2(\text{high})$ vibration mode has a similar frequency for the undoped GaN and Mg-Zn co-doped GaN powders, with a value of 557.38 cm^{-1} . The vibration mode $A_1(\text{TO})$ for undoped GaN powders had a frequency of 525.34 cm^{-1} , while the vibration mode $A_1(\text{TO})$ for Mg-Zn co-doped GaN powders was 521.15 cm^{-1} , which depicts a slight shift to the left of 4.19 cm^{-1} for the Mg-Zn co-doped GaN powders compared to undoped GaN powders. This slight shift of the phononic vibration mode could be related to the incorporation by the diffusion of magnesium and zinc co-dopants atoms into GaN [24,25]. Furthermore, a shoulder was located at 648.05 cm^{-1} (Figure 10b), which also might be indicative of the incorporation of magnesium and zinc co-dopants atoms into GaN powders.

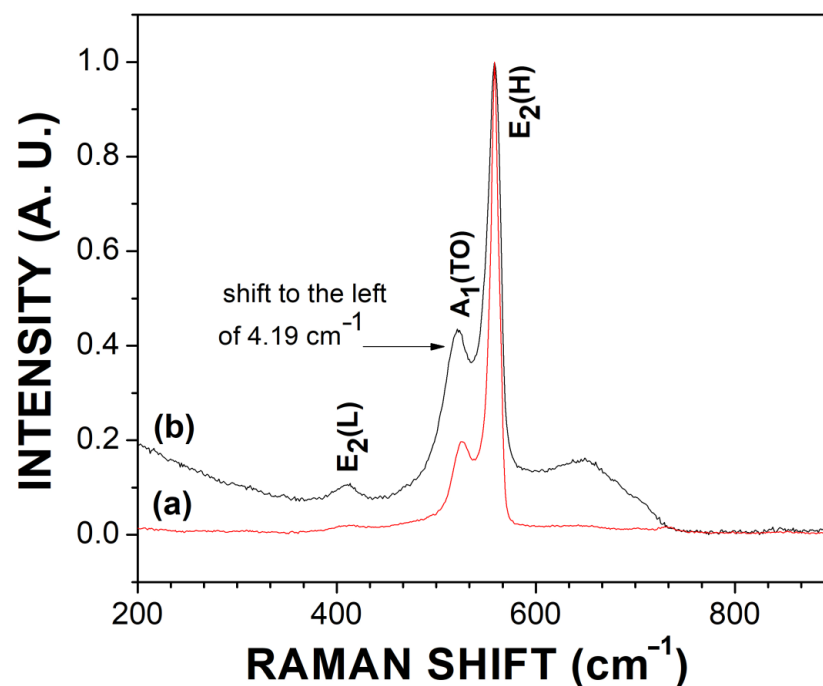


Figure 10. (a) Raman scattering of the undoped GaN powders; (b) Raman scattering of the Mg-Zn co-doped GaN powders.

4. Conclusions

Mg-Zn co-doped GaN powders were obtained via nitridation of a metallic solution of Ga-Mg-Zn at 1000 °C for two hours in ammonia flow. XRD diffraction patterns for Mg-Zn co-doped Ga powders showed a crystal size average of 46.88 nm, with a shift towards greater angles compared to undoped GaN powders. The SEM micrographs demonstrated an irregular shape with a ribbon-like structure and an average length of 8.63 µm for Mg-Zn co-doped GaN powders. EDS showed the presence of zinc (L α 1.012 eV) and magnesium (K α 1.253 eV) as co-dopants atoms, while XPS characterization showed the presence of elemental contributions of magnesium (49.31 eV) and zinc (1019.49 eV), which agree with the EDS analysis. TEM micrographs showed a greater scattering of impurity atoms for the Mg-Zn co-doped GaN powders compared to undoped GaN powders. The photoluminescence spectrum for Mg-Zn co-doped GaN powders showed two fundamental emissions: the first emission located at 3.40 eV (364.70 nm) related to band-to-band transition for hexagonal GaN and a second emission located in a range from 2.80 eV to 2.90 eV (442.85–427.58 nm), which are values characteristics of Mg-doped GaN and Zn-doped GaN powders. Raman scattering demonstrated a shoulder at 648.05 cm⁻¹, which could indicate the incorporation of the Mg and Zn co-dopants atoms into the GaN structure.

Author Contributions: Conceptualization, E.G.; methodology, formal analysis, investigation, writing—original draft, and resources, R.G.; formal analysis, investigation, and writing—original draft, A.M.H.; resources, A.R.; conceptualization, G.G.; resources, G.A.H.; resources, J.A.L.; resources, R.C.C.; writing—original draft, J.A.R.; resources, M.R.; validation, Y.D.R.; and resources, G.M. All authors have read and agreed to the published version of the manuscript.

Funding: This research received no external funding.

Institutional Review Board Statement: Not applicable.

Informed Consent Statement: Not applicable.

Data Availability Statement: Data are contained within the article.

Acknowledgments: The authors gratefully acknowledge the technical support of CNyN-UNAM, particularly Eloísa Aparicio, and Oscar Edel Contreras. This research was partially supported by CONACyT (México), DIFUS-UNISON, and CIDS-ICUAP-BUAP.

Conflicts of Interest: The authors declare no conflict of interest.

References

1. Mohammad, W.; Elomri, A.; Kerbache, L. The global semiconductos chip shortage: Causes, implications, and potential remedies. *IFAC PapersOnLine* **2022**, *10*, 476–483. [[CrossRef](#)]
2. Gastellóu, E.; García, R.; Herrera, A.M.; Ramos, A.; García, G.; Hirata, G.A.; Brown, F.; Morales, C.; Luna, J.A.; Rodríguez, J.A.; et al. Optical and structural analysis of GaN microneedle crystal obtained via GaAs substrates decomposition and their possible growth model using the Volmer-Weber mechanism. *Phys. Status. Solidi. B* **2022**, *260*, 2200201. [[CrossRef](#)]
3. Amano, H.; Baines, Y.; Beam, E.; Borga, M.; Bouchet, T.; Chalker, P.R.; Charles, M.; Chen, K.J.; Chowdhury, N.; Chu, R.; et al. The 2018 GaN power electronics roadmap. *J. Phys. D Appl. Phys.* **2018**, *51*, 1–49. [[CrossRef](#)]
4. Zhao, Y.; Tanaka, S.; Pan, C.-C.; Fujito, K.; Feezell, D.; Speck, J.S.; Denbaars, S.; Nakamura, S. High-power blue-violet semipolar (2021) InGaN/GaN light-emitting diodes with low efficiency droop at 200 A/cm². *Appl. Phys. Express* **2011**, *4*, 082104. [[CrossRef](#)]
5. Liu, X.; Popa, D.; Akhmediev, N. Revealing the transition dynamics from Q switching to mode locking in a soliton laser. *Phys. Rev. Lett.* **2019**, *123*, 093901. [[CrossRef](#)]
6. Guan, M.; Chen, D.; Hu, S.; Zhao, H.; You, P.; Meng, S. Theoretical insights into ultrafast dynamics in quantum materials. *Ultrafast Sci.* **2022**, *2022*, 976725. [[CrossRef](#)]
7. Li, X.; Huang, X.; Han, Y.; Chen, E.; Guo, P.; Zhang, W.; An, M.; Pan, Z.; Xu, Q.; Guo, X.; et al. High-performance γ -MnO₂ dual-core, pair-hole fiber for ultrafast photonics. *Ultrafast Sci.* **2023**, *3*, 0006. [[CrossRef](#)]
8. Liu, X.; Pang, M. Revealing the buildup dynamics of harmonic mode-locking states in ultrafast lasers. *Laser Photonics Rev.* **2019**, *13*, 1800333. [[CrossRef](#)]
9. Zhang, Z.; Zhang, J.; Chen, Y.; Xia, T.; Wang, L.; Han, B.; He, F.; Sheng, Z.; Zhang, J. Bessel terahertz pulses from superluminal laser plasma filaments. *Ultrafast Sci.* **2022**, *2022*, 9870325. [[CrossRef](#)]
10. Li, X.; Xu, W.; Wang, Y.; Zhang, X.; Hui, Z.; Zhang, H.; Wageh, S.; Al-Hartomy, O.A.; Al-Sehemi, A.G. Optical-intensity modulators with PbTe thermoelectric nanopowders for ultrafast photonics. *Appl. Mater. Today* **2022**, *28*, 101546. [[CrossRef](#)]

11. Zhang, J.; Tse, K.; Wong, M.; Zhang, Y.; Zhu, J. A brief review of co-doping. *Front. Phys. Express* **2016**, *6*, 117405. [[CrossRef](#)]
12. Ploog, K.H.; Brandt, O. Doping of group III nitrides. *J. Vac. Sci. Technol. A* **1998**, *3*, 1609–1614. [[CrossRef](#)]
13. Korotkov, R.Y.; Gregie, J.M.; Wessels, B.W. Electrical properties of p-type GaN: Mg codoped with oxygen. *Appl. Phys. Lett.* **2001**, *78*, 222–224. [[CrossRef](#)]
14. Pan, H.; Gu, B.; Eres, G.; Zhang, Z. Ab initio study on noncompensated Cr codoping of GaN for enhanced solar energy conversion. *J. Chem. Phys.* **2010**, *132*, 104501. [[CrossRef](#)] [[PubMed](#)]
15. Kim, K.S.; Han, M.S.; Yang, G.M.; Youn, C.J.; Lee, H.J.; Cho, H.K.; Lee, J. Codoping characteristics of Zn with Mg in GaN. *Appl. Phys. Lett.* **2000**, *77*, 1123–1125. [[CrossRef](#)]
16. Kim, K.S.; Oh, C.S.; Han, M.S.; Kim, C.S.; Yang, G.M.; Yang, J.W.; Hong, C.H.; Youn, C.J.; Lim, K.Y.; Lee, H.J. Co-doping characteristics of Si and Zn with Mg in P-type GaN. *Mater. Res. Soc. Internet J. Nitride Semicond. Res.* **1999**, *595*, 384. [[CrossRef](#)]
17. Gastellóu, E.; Morales, C.; García, R.; García, G.; Hirata, G.A.; Galeazzi, R.; Herrera, A.M.; Rosendo, E.; Díaz, T.; Ramos, J.R.; et al. Coypol, enhanced crystalline size of undoped GaN powders obtained by nitridation of metallic gallium. *Opt. Mater.* **2018**, *83*, 220–224. [[CrossRef](#)]
18. Ghasemi, M.; Johansson, J. Thermodynamic assessment of the As-Zn and As-Ga-Zn systems. *J. Alloys Compd.* **2015**, *638*, 95–102. [[CrossRef](#)]
19. Dutkiewicz, J.; Moser, Z.; Zabdyr, L.; Gohil, D.D.; Chart, T.G.; Ansara, I.; Girard, C. The Ga-Zn (Gallium-Zinc) system. *Bull. Alloy. Phase Diagr.* **1990**, *11*, 77–82. [[CrossRef](#)]
20. Okamoto, H. Ga-Mg (Gallium-Magnesium). *J. Phase Equilib.* **1991**, *12*, 119–120. [[CrossRef](#)]
21. Meng, F.-G.; Wang, J.; Rong, M.-H.; Liu, L.-B.; Jin, Z.-P. Thermodynamic assessment of Ga-Mg binary system. *Trans. Nonferrous Met. Soc. China* **2010**, *20*, 450–457. [[CrossRef](#)]
22. Langford, J.I.; Wilson, A.J.C. Sherrer after sixty years: A survey and some new results in the determination of crystallite size. *J. Appl. Cryst.* **1978**, *11*, 102–113. [[CrossRef](#)]
23. Reshchikov, M.A.; Morkoç, H. Luminescence properties of defects in GaN. *J. Appl. Phys.* **2005**, *97*, 061301. [[CrossRef](#)]
24. Gastellóu, E.; Morales, C.; García, R.; García, G.; Hirata, G.A.; Herrera, A.M.; Galeazzi, R.; Rosendo, E.; Díaz, T.; Tejada, E.M. P-type GaN powders obtained by nitridation of Ga-Mg liquid metallic solution. *J. Alloys Compd.* **2019**, *772*, 1024–1029. [[CrossRef](#)]
25. Gastellóu, E.; Morales, C.; García, G.; García, R.; Hirata, G.A.; Herrera, A.M.; Galeazzi, R.; Rosendo, E.; Díaz, T. Zinc doping of Ga-rich GaN powders obtained by nitridation of the Ga-Zn liquid metallic solution. *J. Alloys Compd.* **2019**, *738*, 927–934. [[CrossRef](#)]

Disclaimer/Publisher’s Note: The statements, opinions and data contained in all publications are solely those of the individual author(s) and contributor(s) and not of MDPI and/or the editor(s). MDPI and/or the editor(s) disclaim responsibility for any injury to people or property resulting from any ideas, methods, instructions or products referred to in the content.